Thermally activated bipyridyl-based Mn-MOF with Lewis acid-base bifunctional sites for highly efficient catalytic cycloaddition of CO_2 with epoxides and Knoevenagel condensation reaction

Zhen Xu,[a] Ya-Yu Zhao,[a] Le Chen,[a] Cai-Yong Zhu,[a] Peng Li,[a] Wei Gao,*[a] Ji-Yang Li,[b] and Xiu-Mei Zhang*[a]

Table S1. Selected bond lengths (Å) and angles (°) for Mn-MOF-**1**.

Mn1-O3A	2.158(6)	O3B-Mn1-N1D	90.6(2)
Mn1-O3B	2.158(6)	O1-Mn1-N1D	89.6(2)
Mn1-O1	2.173(6)	O1C-Mn1-N1D	89.6(2)
Mn1-O1C	2.173(6)	O3A-Mn1-O5	89.5(2)
Mn1-N1D	2.246(9)	O3B-Mn1-O5	89.5(2)
Mn1-O5	2.248(9)	O1-Mn1-O5	90.3(2)
Mn2-O7	2.091(8)	O1C-Mn1-O5	90.3(2)
Mn2-O4E	2.148(6)	N1D-Mn1-O5	179.9(3)
Mn2-O4F	2.148(6)	O7-Mn2-O4E	97.3(2)
Mn2-O6	2.165(9)	O7-Mn2-O4	97.3(2)
Mn2-O2C	2.282(6)	O4E-Mn2-O4F	93.9(4)
Mn2-O2	2.282(6)	O7-Mn2-O6	172.8(4)
O3-Mn1B	2.158(6)	O4E-Mn2-O6	87.6(3)
O4-Mn2E	2.148(6)	O4F-Mn2-O6	87.6(3)
N1-Mn1D	2.246(9)	O7-Mn2-O2C	87.9(2)
		O4E-Mn2-O2C	172.2(2)
O3A-Mn1-O3B	90.3(3)	O4F-Mn2-O2C	91.2(2)
O3A-Mn1-O1	179.7(2)	O6-Mn2-O2C	86.7(3)
O3B-Mn1-O1	89.5(2)	O7-Mn2-O2	87.9(2)
O3A-Mn1-O1C	89.5(2)	O4E-Mn2-O2	91.2(2)
O3B-Mn1-O1C	179.7(2)	O4F-Mn2-O2	172.2(2)
O1-Mn1-O1C	90.8(3)	O6-Mn2-O2	86.7(3)

O3A-Mn1-N1D	90.6(2)	O2C-Mn2-O2	83.2(3)

Symmetry codes: A -x+1/2, y-1/2, -z+1; B -x+1/2, -y+1/2, -z+1; C x, -y, z; D -x, -y ,-z; E -x+1/2, -y+1/2, -z+2; F -x+1/2, y-1/2, -z+2.

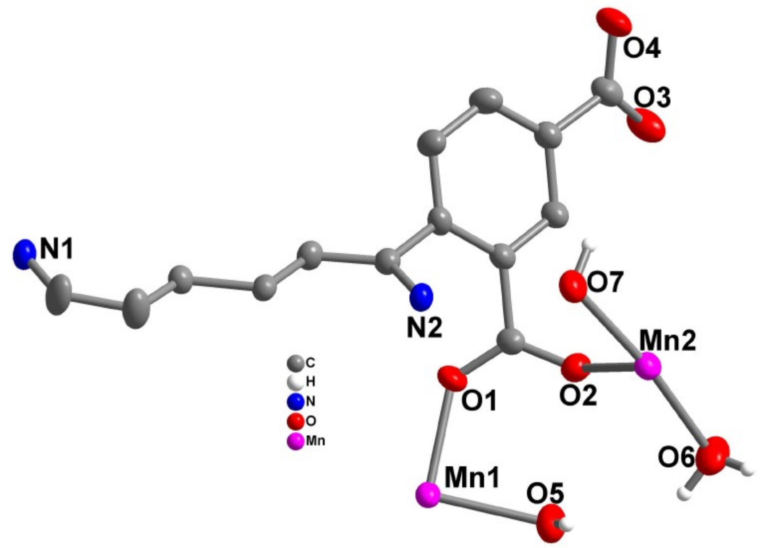

Fig. S1 A view of asymmetric unit of Mn-MOF-**1** with thermal ellipsoids drawn at the 50 % probability level.

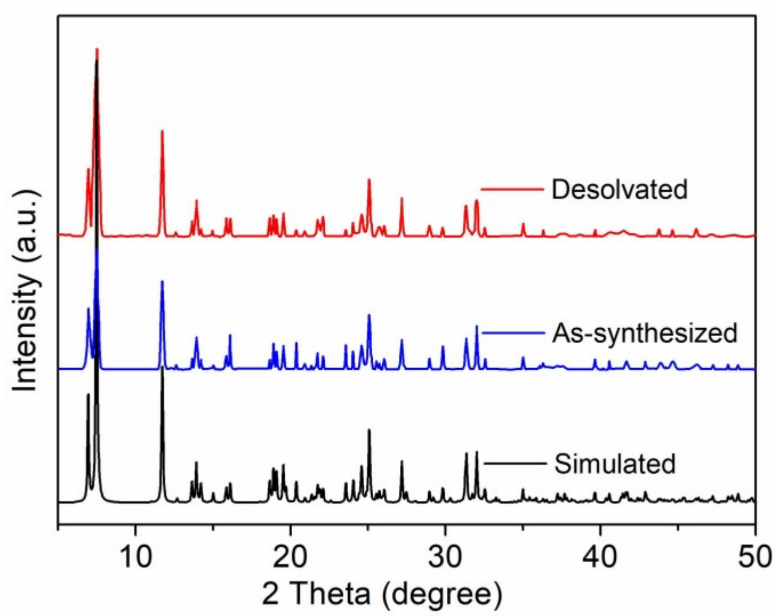

Fig. S2 PXRD patterns of simulated, as-synthesized, and activated Mn-MOF-**1**.

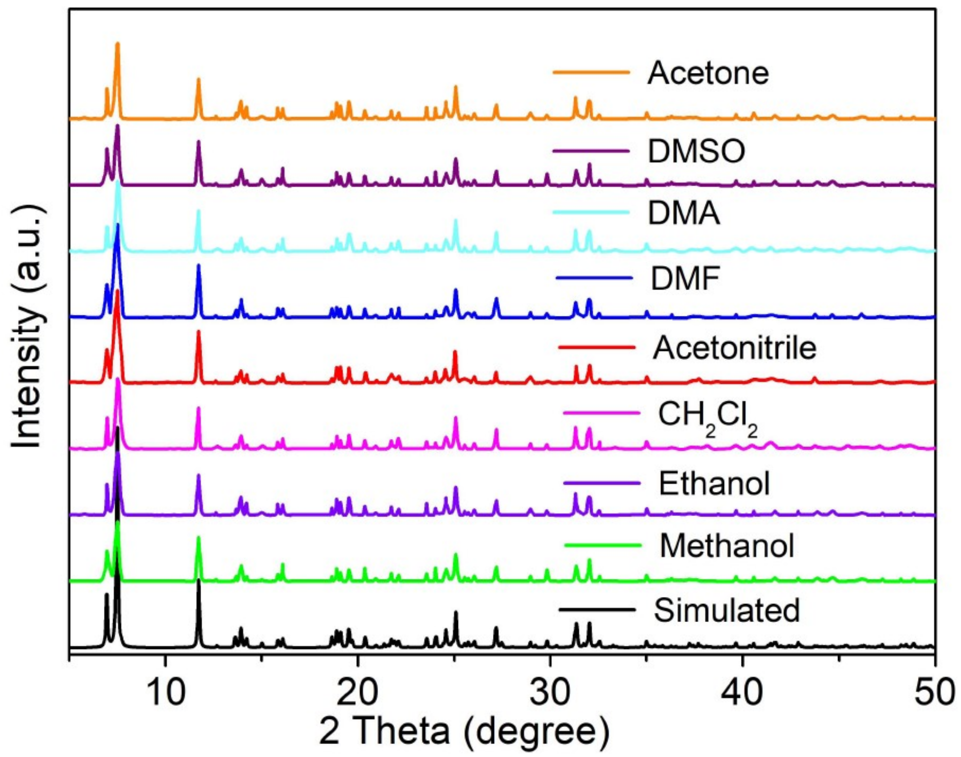

Fig. S3 The PRXD patterns of Mn-MOF-**1** samples immersed in different solvents and simulated crystal data.

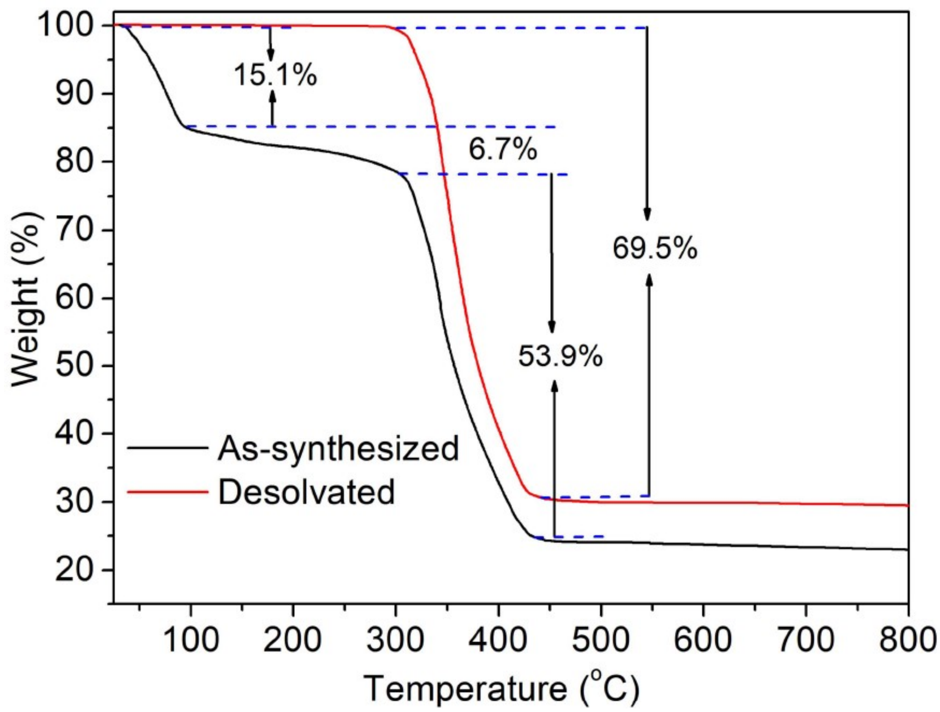

Fig. S4 TGA spectra of as-synthesized and activated Mn-MOF-**1**

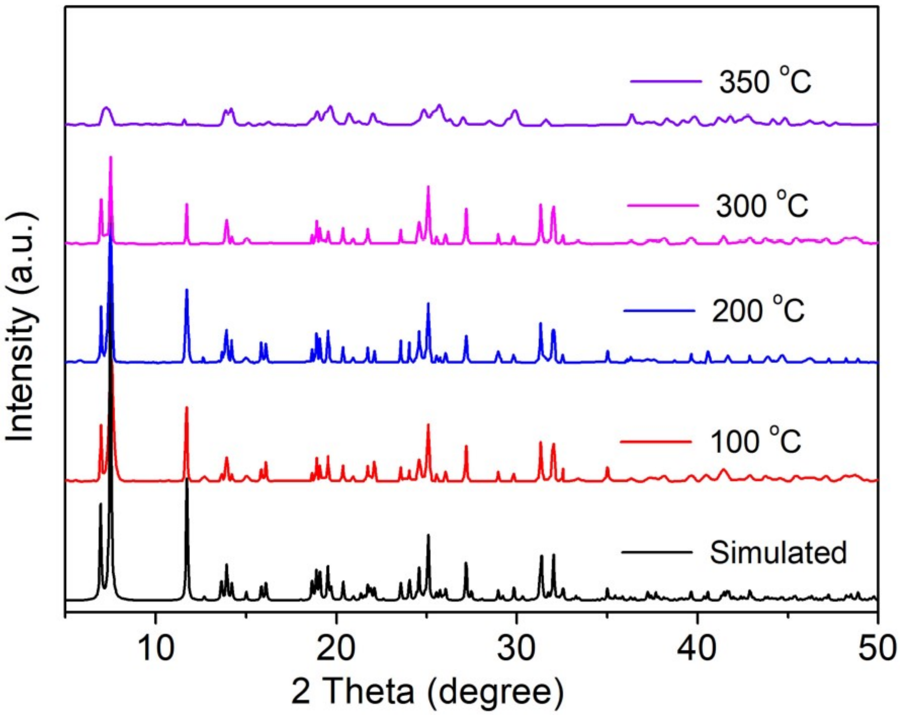

Fig. S5 The PRXD patterns of Mn-MOF-**1** samples heated in different temperature and simulated crystal data.

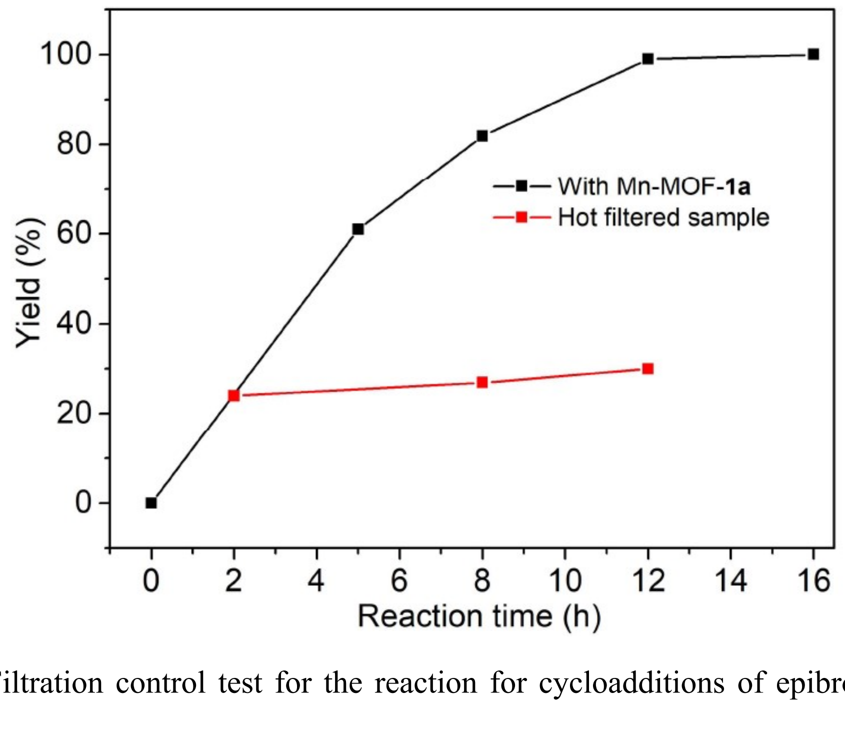

Fig. S6 Filtration control test for the reaction for cycloadditions of epibromohydrin with CO_2.

Table S2 Comparison of Mn-MOF-**1** with other MOF-based catalysts for the cycloaddition of CO_2 with epibromohydrin.

Entry	Catalyst	Catalyst (mol %)[a]	$n\text{-}Bu_4NBr$ (mol %)	P (atm)	t (h)	T (°C)	Yield (%)	TON[b]	Refs
1	$\{[Cd(Hbptc)]\cdot H_2O\}_n$	0.1	1	1	4	80	95	400	S1
2	$[Zn_2(TCA)(BIB)_{2.5}]\cdot(NO_3)$	0.5	1	1	4	80	99	200	S3
3	$\{[(CH_3)_2NH_2]_2[CaZn(TDP)(H_2O)]\cdot 3DMF\cdot 3H_2O\}_n$	2	5	1	6	60	99	50	S4
4	$\{[Cu_2(F\text{-}ptta)(H_2O)_2]\cdot 5DMF\cdot 2H_2O\}n$	0.3	4	1	8	60	99	330	S5
5	$\{[Zn(dibpca)(OAc)]\cdot 2.5H_2O\}_n$	0.1	2.5	1	48	25	90	900	S7
6	$[Zn_2(iso)_2(bpy)_2]_n$	0.41	0.84	2	2	80	98.2	244	S8
7	$\{2Cu(L)(A)\cdot 3H_2O\}_n$	0.2	6	1	24	90	96	480	S9
8	$[Zn(L)(bpa)_{0.5}]_n$	1	10	1	6	40	99	100	S10
9	Mn-MOF-**1**	0.38	0.4	4	12	80	99	266	This work

[a]Catalyst amount relative to the epoxide. [b]product (mmol)/catalyst (mmol).

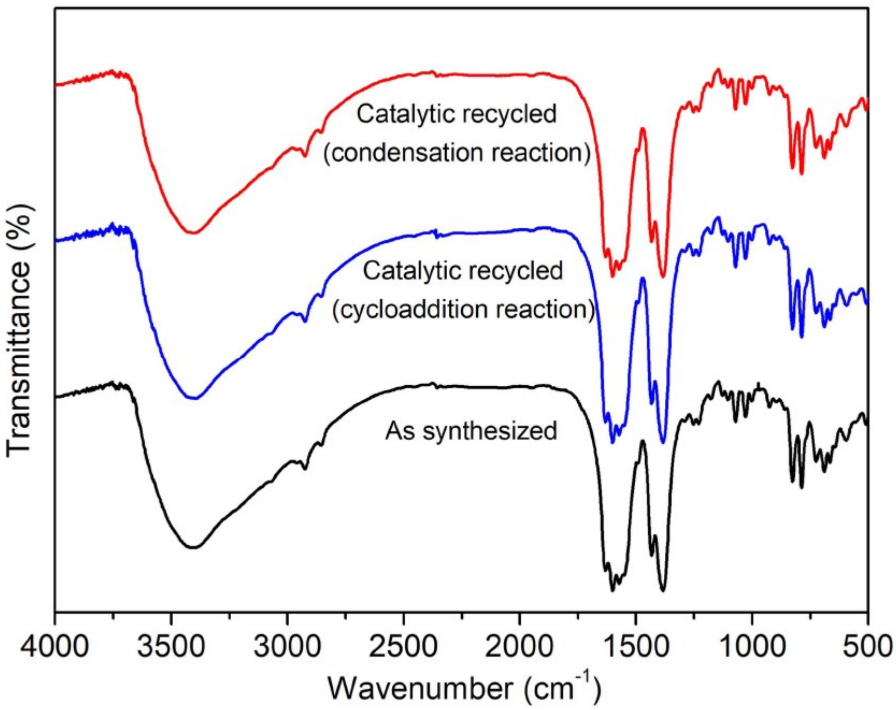

Fig. S7 FT-IR spectra of Mn-MOF-**1** catalyst before and after catalysis.

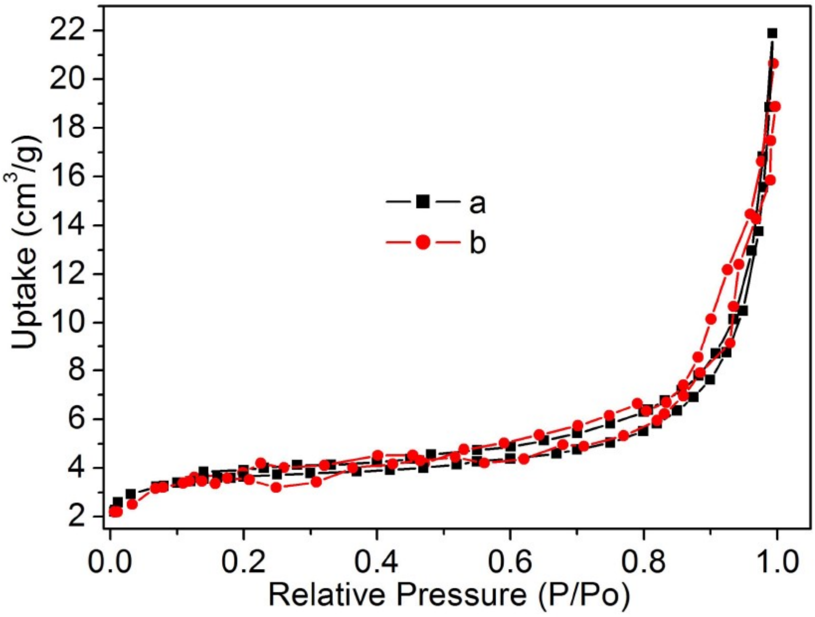

Fig. S8 N_2 adsorption-desorption isotherms of Mn-MOF-**1a** before (a) and after (b) catalytic cycloaddition of CO_2 with epibromohydrin.

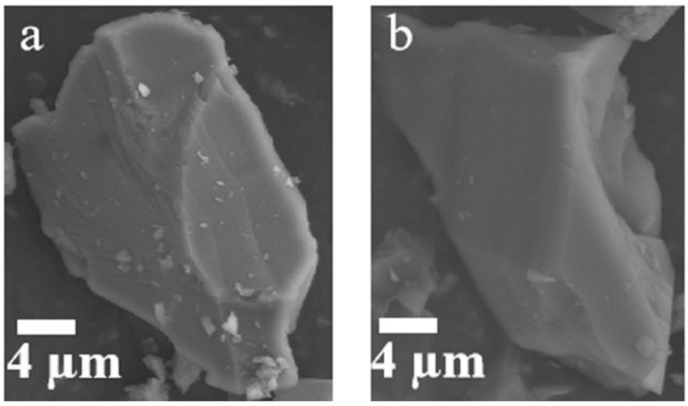

Fig. S9 The SEM imagines of Mn-MOF-**1** before (a) and after (b) catalytic cycloaddition of CO_2 with epibromohydrin.

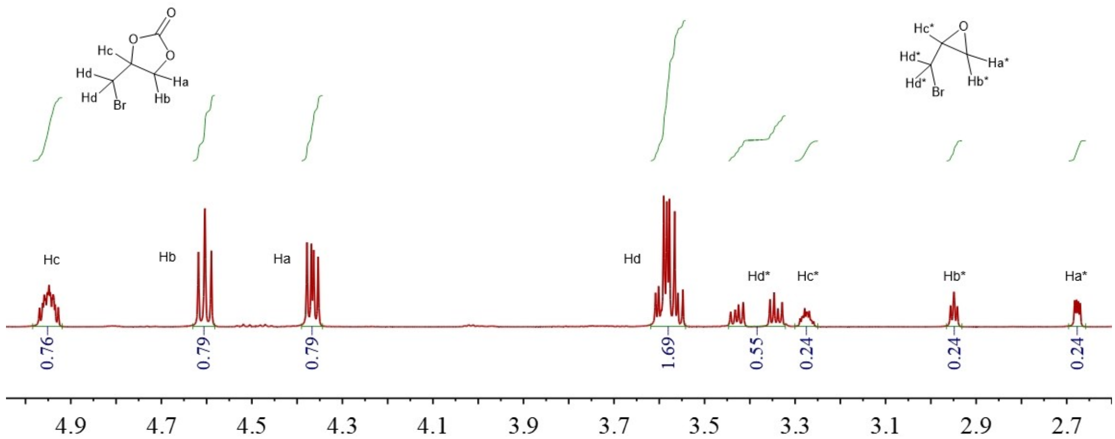

Fig. S10 The comparison of [1]H NMR spectra of epibromohydrin and its related catalytic product. (Yield: 76 % **Table 2** entry 8).

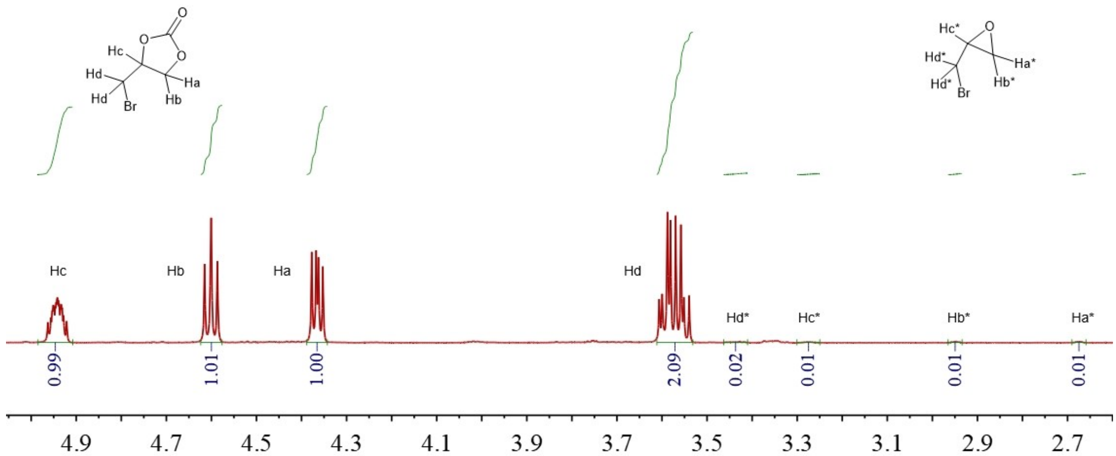

Fig. S11 The comparison of [1]H NMR spectra of epibromohydrin and its related catalytic product. (Yield: 99 % **Table 2** entry 9).

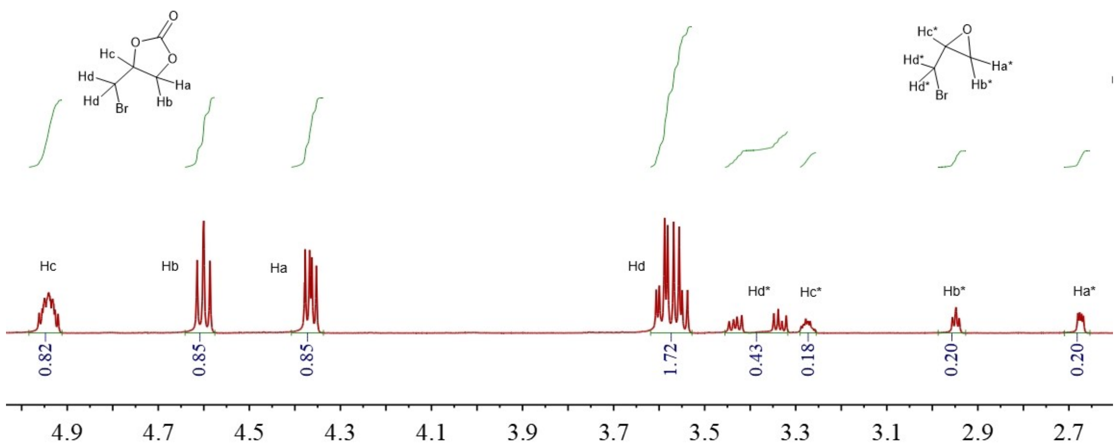

Fig. S12 The comparison of [1]H NMR spectra of epibromohydrin and its related catalytic product. (Yield: 82 % **Table 2** entry 12).

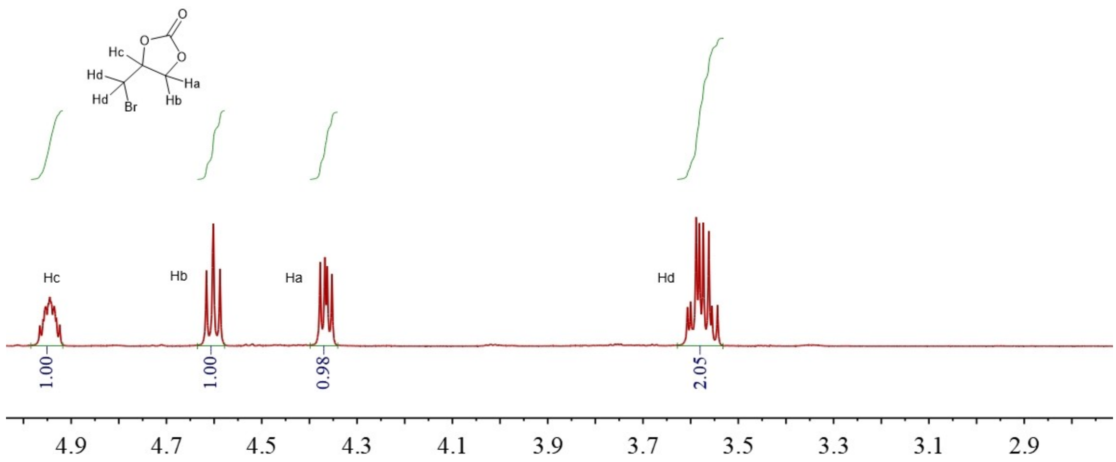

Fig. S13 The comparison of ^{1}H NMR spectra of epibromohydrin and its related catalytic product. (Yield: 100 % **Table 2** entry 13).

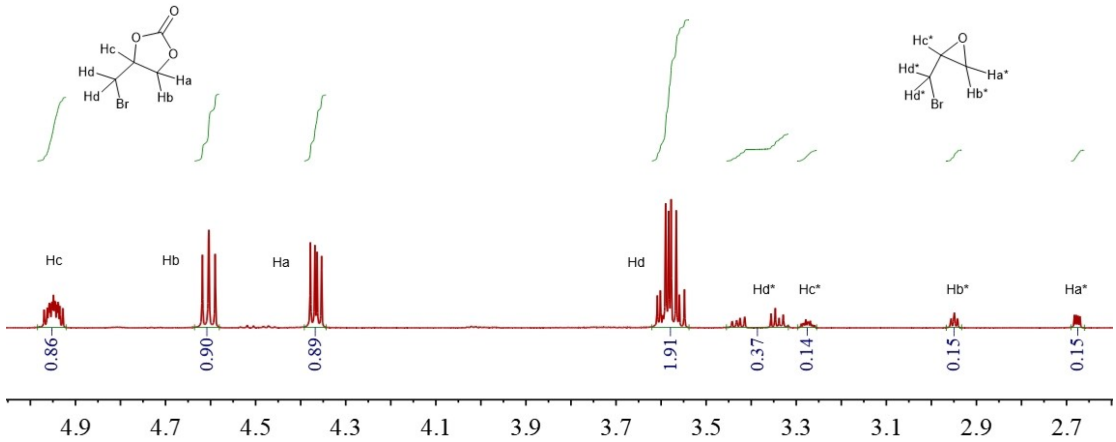

Fig. S14 The comparison of ^{1}H NMR spectra of epibromohydrin and its related catalytic product. (Yield: 86 % **Table 2** entry 14).

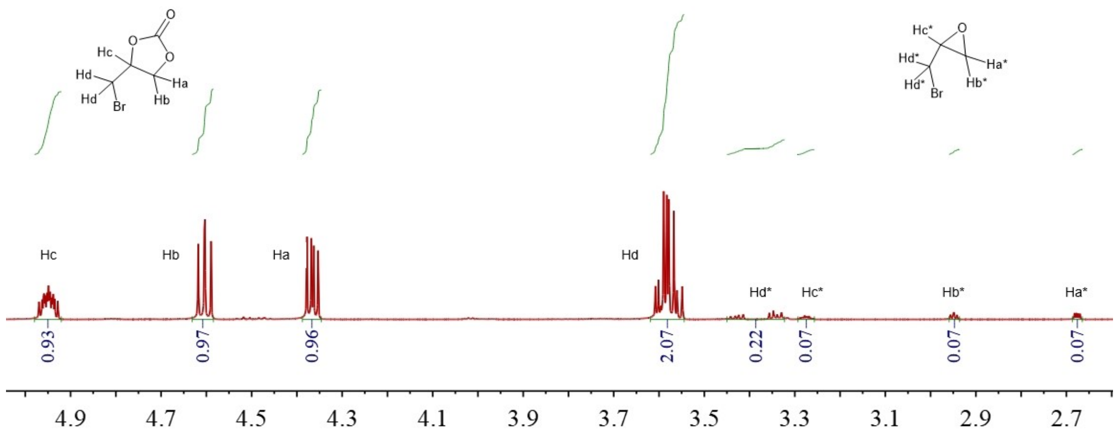

Fig. S15 The comparison of ^{1}H NMR spectra of epibromohydrin and its related catalytic product. (Yield: 93 % **Table 2** entry 15).

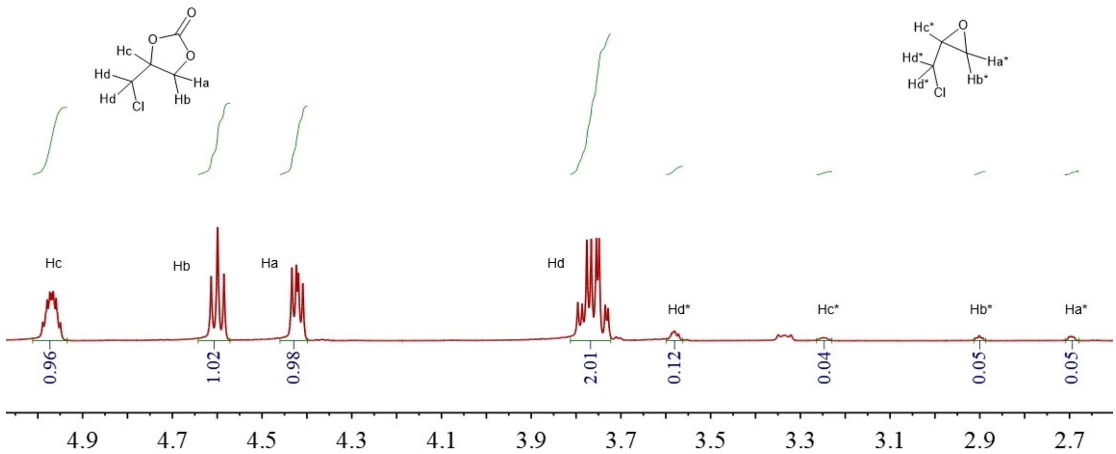

Fig. S16 The comparison of ^{1}H NMR spectra of epichlorohydrin and its related catalytic product. (Yield: 96 % **Table 3** entry 2).

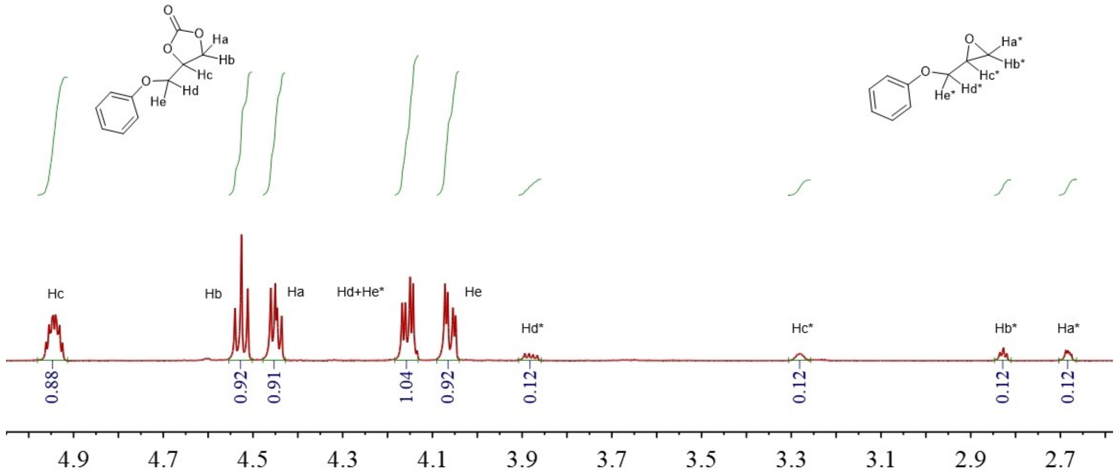

Fig. S17 The comparison of ^{1}H NMR spectra of phenyl glycidyl ether and its related catalytic product. (Yield: 88 % **Table 3** entry 3 for12 h).

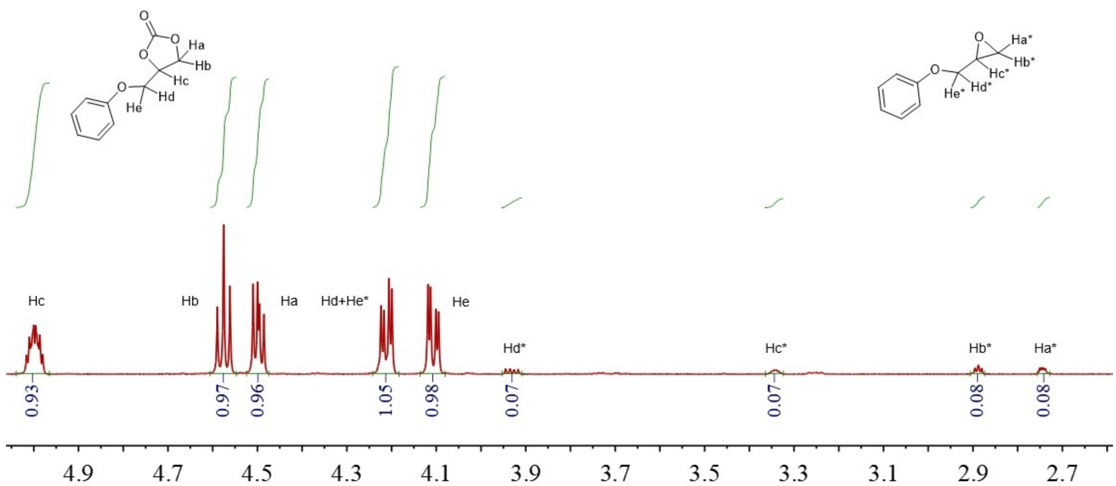

Fig. S18 The comparison of ^{1}H NMR spectra of phenyl glycidyl ether and its related catalytic product. (Yield: 93 % **Table 3** entry 3 for16 h).

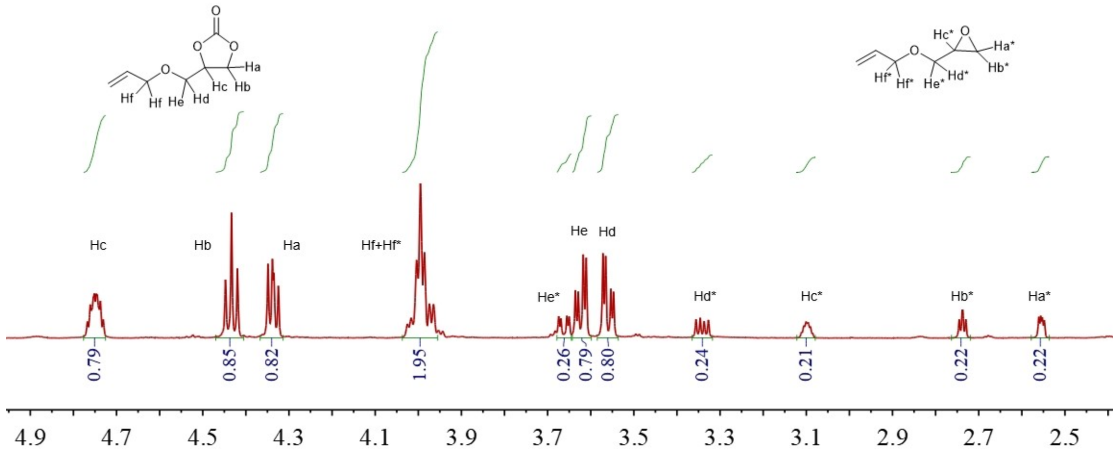

Fig. S19 The comparison of ^{1}H NMR spectra of allyl glycidyl ehter and its related catalytic product. (Yield: 79 % **Table 3** entry 4 for12 h).

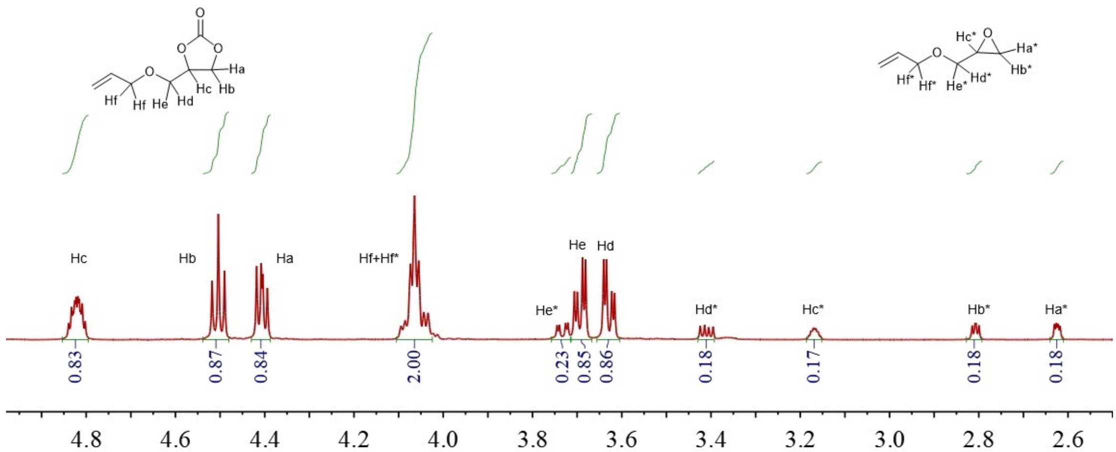

Fig. S20 The comparison of ^{1}H NMR spectra of allyl glycidyl ehter and its related catalytic product. (Yield: 83 % **Table 3** entry 4 for16 h).

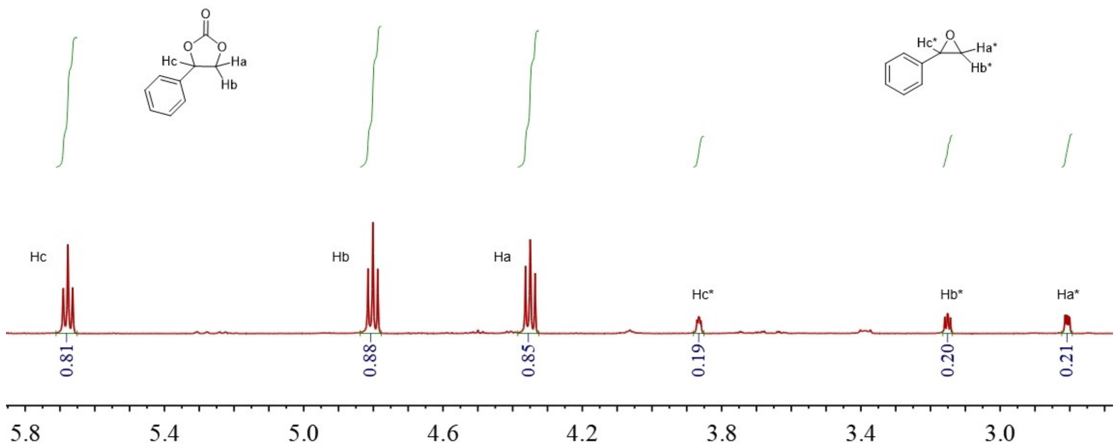

Fig. S21 The comparison of ^{1}H NMR spectra of styrene oxide and its related catalytic product. (Yield: 81 % **Table 3** entry 5 for12 h).

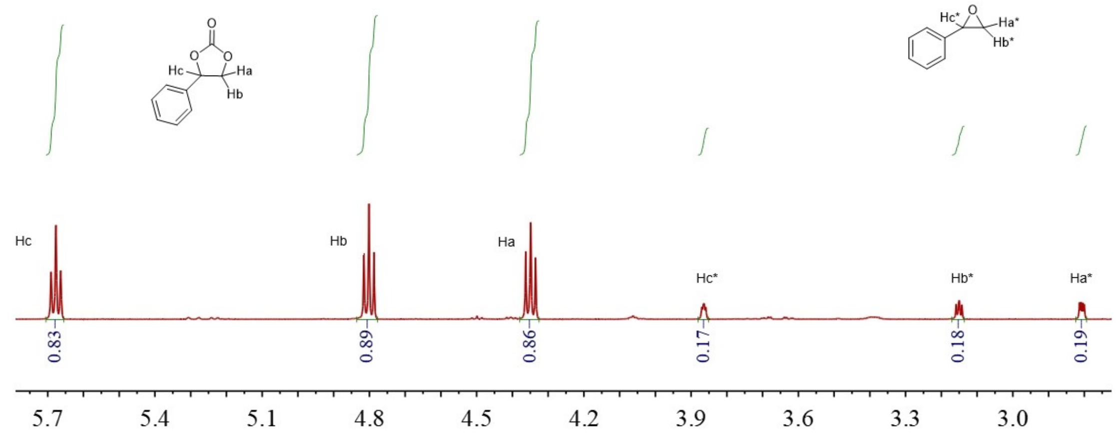

Fig. S22 The comparison of [1]H NMR spectra of styrene oxide and its related catalytic product. (Yield: 83 % **Table 3** entry 5 for16 h).

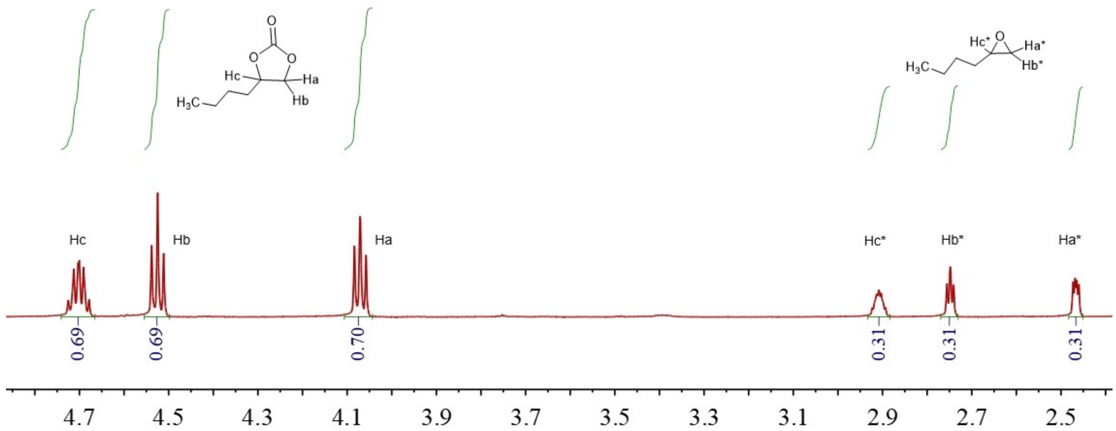

Fig. S23 The comparison of [1]H NMR spectra of epoxyhexane and its related catalytic product. (Yield: 69 % **Table 3** entry 6 for12 h).

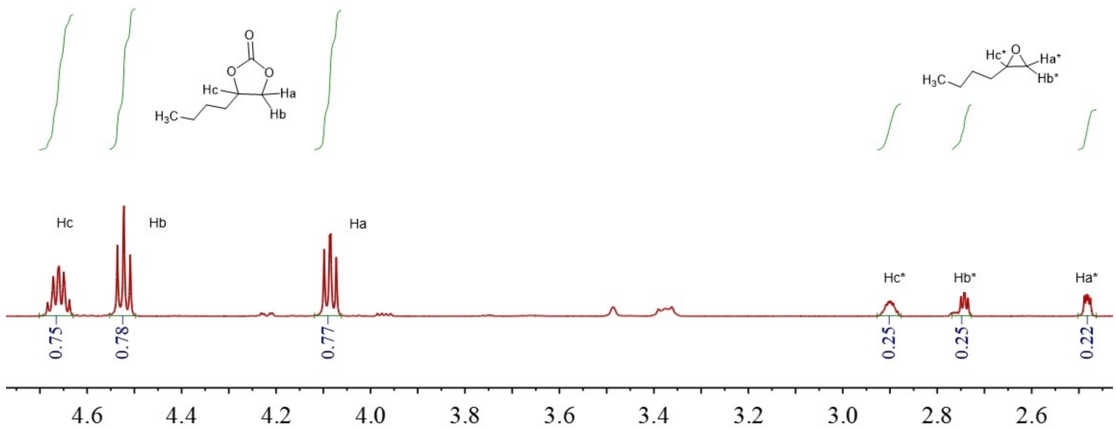

Fig. S24 The comparison of [1]H NMR spectra of epoxyhexane and its related catalytic product. (Yield: 75 % **Table 3** entry 6 for16 h).

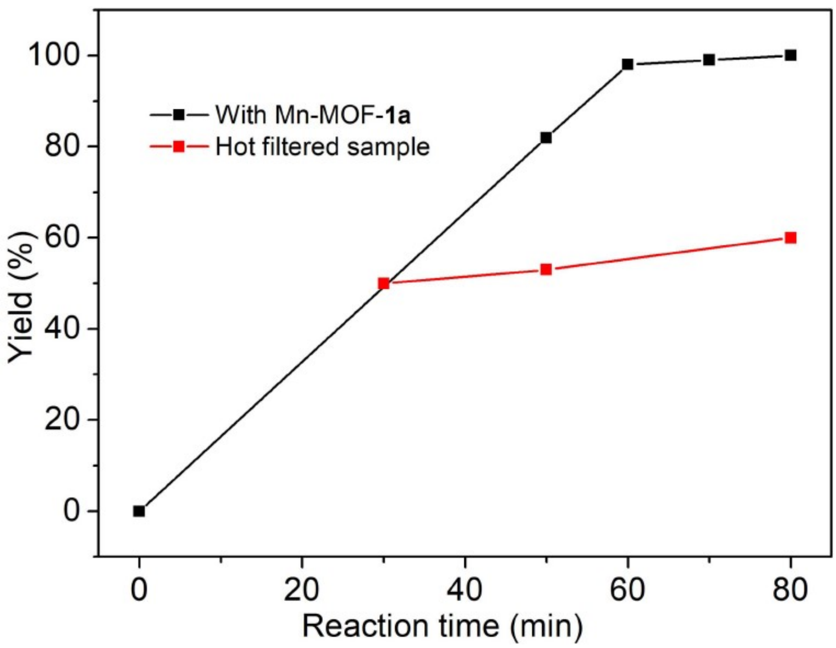

Fig. S25 Filtration control test for the reaction for the Knoevenagel condensation reaction of benzaldehyde.

Table S3 Comparison of the catalytic activity of various MOFs for the Knoevenagel condensation reaction of benzaldehyde.

Entry	Catalyst	Catalyst (mol%)[a]	Solvent	t(min)	T(°C)	Yield (%)	TON[b]	TOF[c]	Refs
1	$\{(Me_2NH_2)_2[Mn_2(TDP)(H_2O)_2]\cdot 3H_2O\cdot 3DMF\}_n$	0.3	Ethanol	60	60	99	330	5.5	S9
2	$[Zn(bix)]\{V_2O_6\}$	1	Solvent-free	60	60	99	100	1.67	S10
3	$\{[Ba_3Zn_4(TDP)_2(HCO_2)_2(OH_2)_2]\cdot 7DMF\cdot 4H_2O\}_n$	0.3	Ethanol	60	60	99	330	5.5	S11
4	$\{[Cu_2(\mu_3\text{-pdba})_2(2,2'\text{-bipy})]\cdot 2H_2O\}_n$	2	Methanol	60	25	99	50	0.83	S12
5	$[Co_2(bptc)(H_2O)_2]\cdot 5DMA$	2	Solvent-free	360	60	99.8	50	0.14	S13
6	$Ni_3(BTC)_2(4\text{-TPT})_2(H_2O)_6\cdot 1.5H_2O$	0.25	DMF	360	25	87	348	0.97	S14
7	JNU-402-NH_2	0.6	Solvent-free	60	80	99	166	2.77	S15
8	$[Zn_2(BTC)]_n\cdot 3n(DMF)\cdot 2n(H_2O)$	1	THF	120	25	94	94	0.78	S16
9	Hf-UiO-66-N_2H_3	0.74	Ethanol	240	25	98	132.4	0.55	S17
10	Mn-MOF-**1**	0.75	Ethanol	80	25	99	133.3	1.67	This work

[a]Catalyst amount relative to the benzaldehyde. [b]product (mmol)/catalyst (mmol).[c]product (mmol)/catalyst (mmol) / t (min).

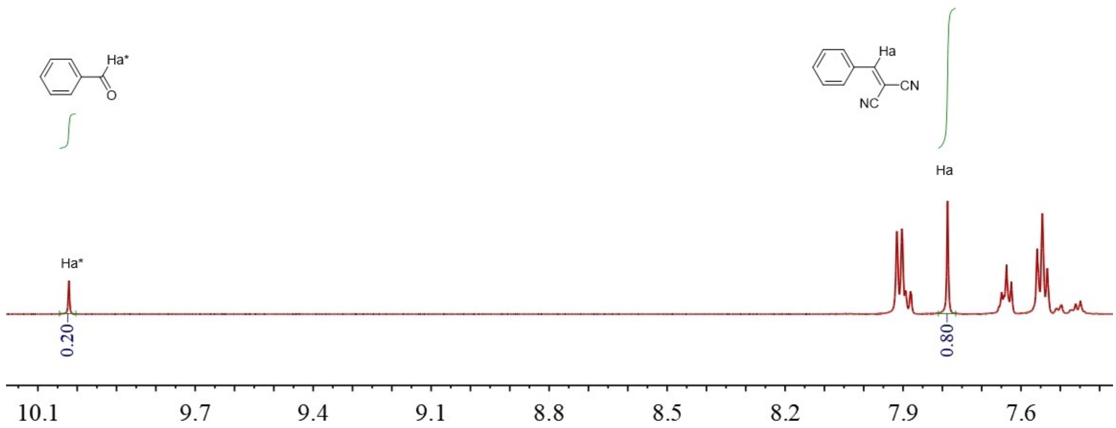

Fig. S26 The comparison of ^{1}H NMR spectra of benzaldehyde and its related catalytic product. (Yield: 80 % **Table 4** entry 2).

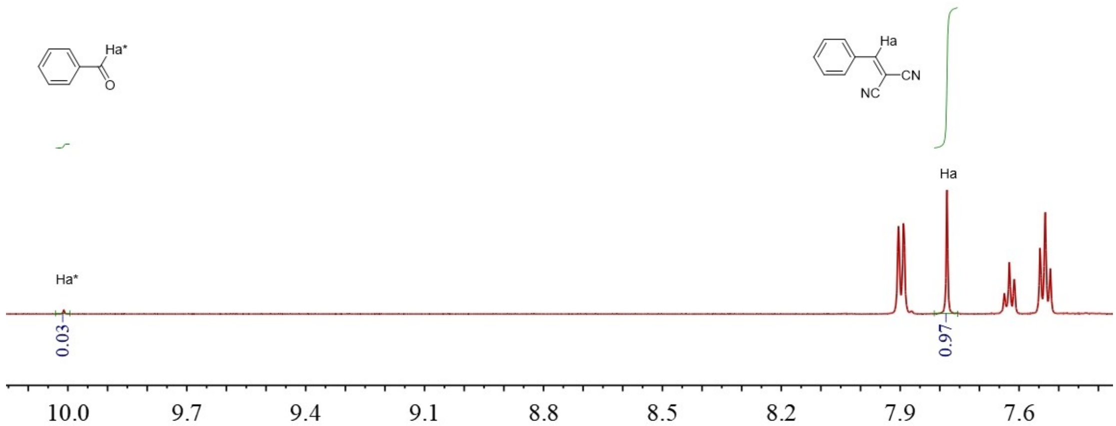

Fig. S27 The comparison of ^{1}H NMR spectra of benzaldehyde and its related catalytic product. (Yield: 97 % **Table 4** entry 3).

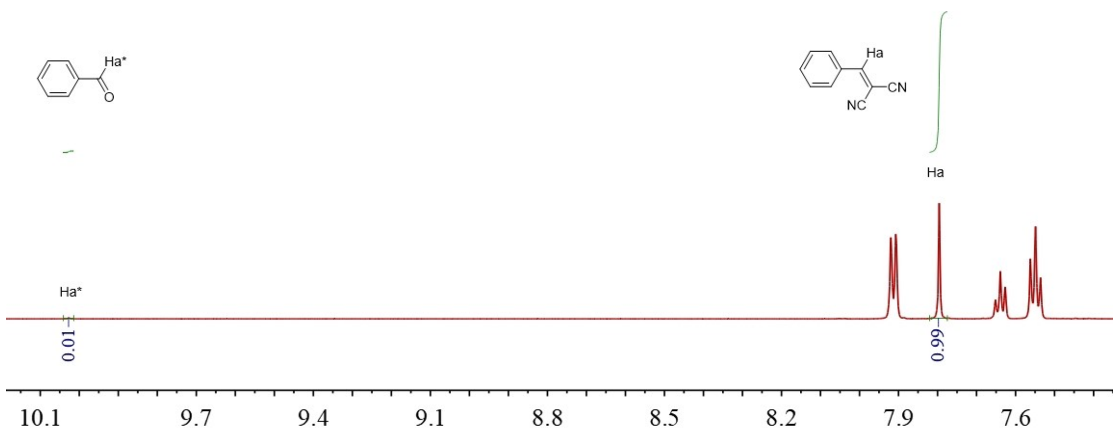

Fig. S28 The comparison of ^{1}H NMR spectra of benzaldehyde and its related catalytic product. (Yield: 99 % **Table 4** entry 4).

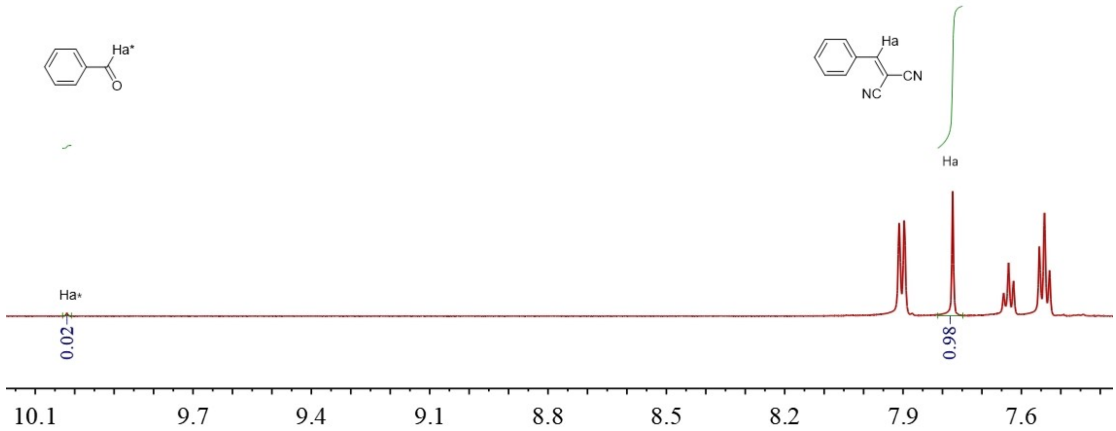

Fig. S29 The comparison of ^{1}H NMR spectra of benzaldehyde and its related catalytic product. (Yield: 98 % **Table 4** entry 5).

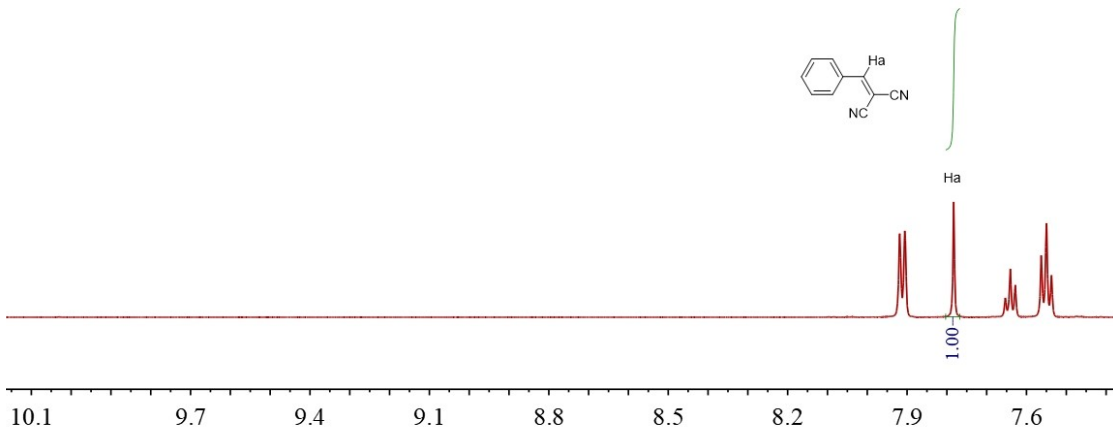

Fig. S30 The comparison of ^{1}H NMR spectra of benzaldehyde and its related catalytic product. (Yield: 100 % **Table 4** entry 8).

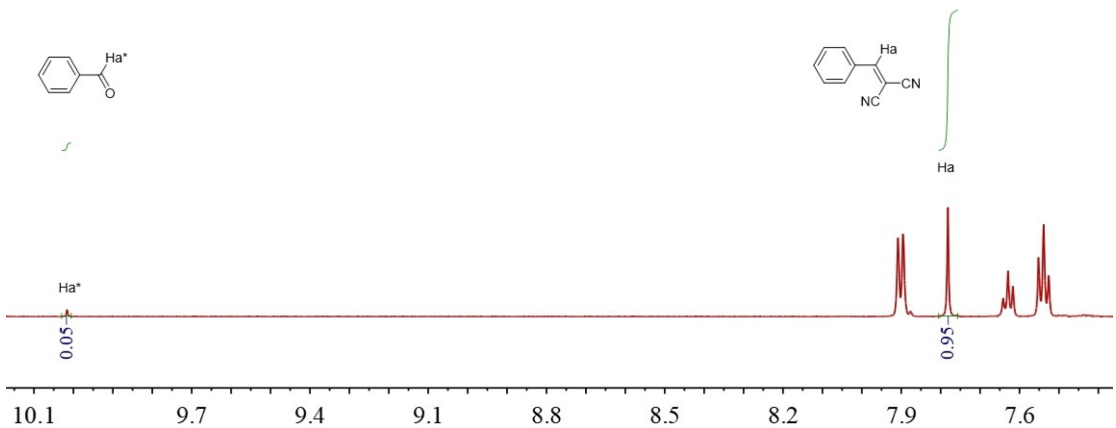

Fig. S31 The comparison of ^{1}H NMR spectra of benzaldehyde and its related catalytic product. (Yield: 95 % **Table 4** entry 9).

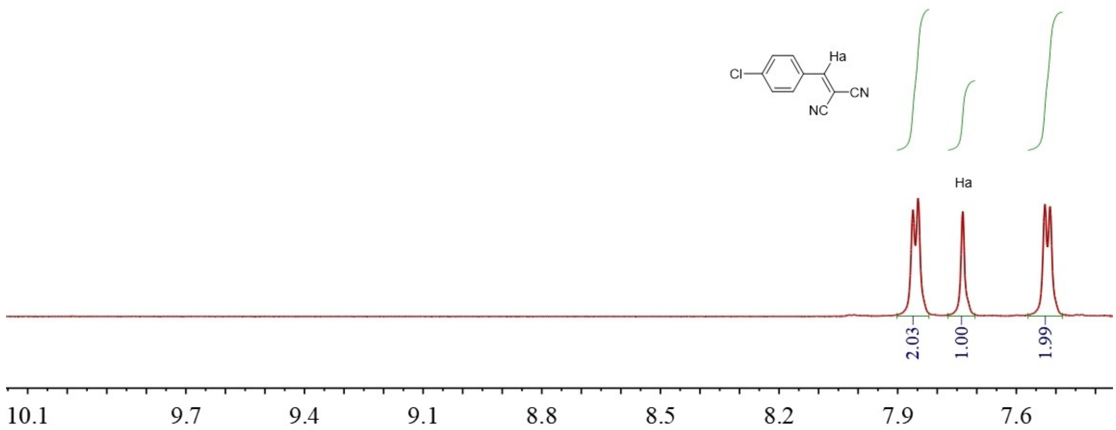

Fig. S32 The comparison of ^{1}H NMR spectra of 4-chlorobenzaldehyde and its related catalytic product. (Yield: >99 % **Table 5** entry 2).

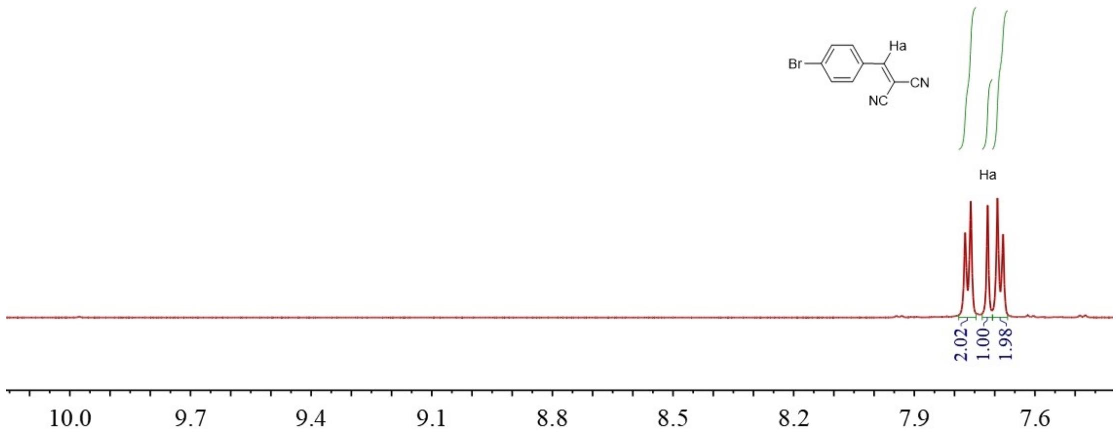

Fig. S33 The comparison of ^{1}H NMR spectra of 4-bromobenzaldehyde and its related catalytic product. (Yield: >99 % **Table 5** entry 3).

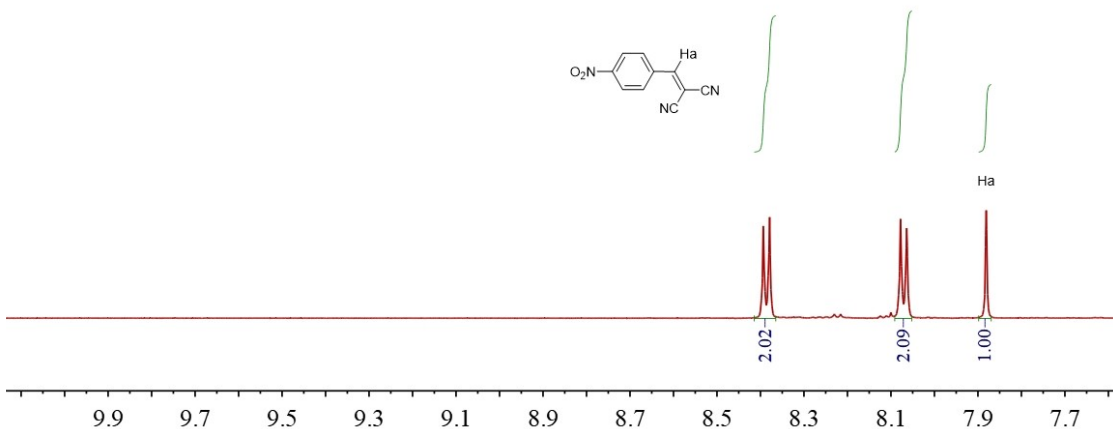

Fig. S34 The comparison of ^{1}H NMR spectra of 4-nitrobenzaldehyde and its related catalytic product. (Yield: >99 % **Table 5** entry 4).

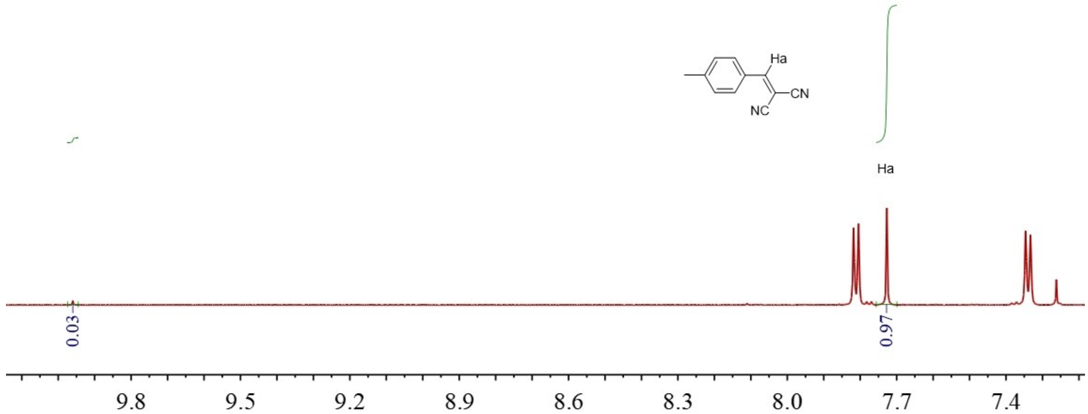

Fig. S35 The comparison of ^{1}H NMR spectra of 4-methylbenzaldehyde and its related catalytic product. (Yield: 97 % **Table 5** entry 5).

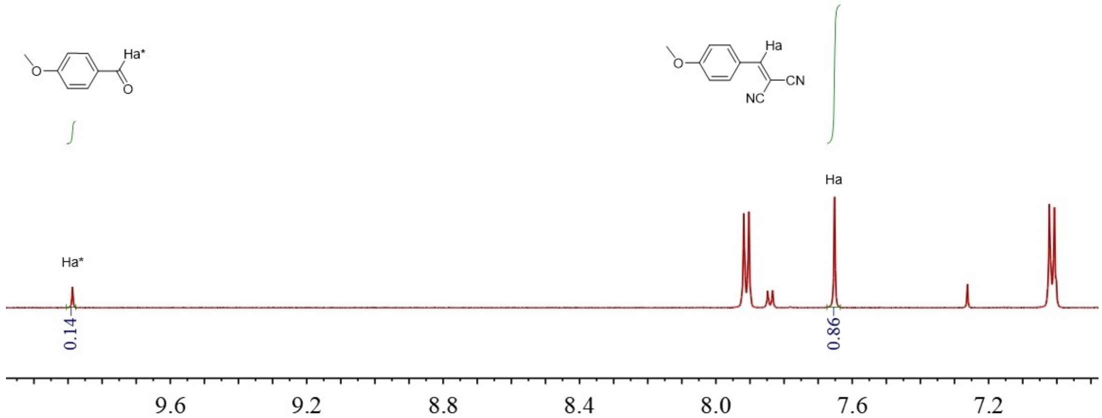

Fig. S36 The comparison of ^{1}H NMR spectra of 4-methoxybenzaldehyde and its related catalytic product. (Yield: 86 % **Table 5** entry 6).

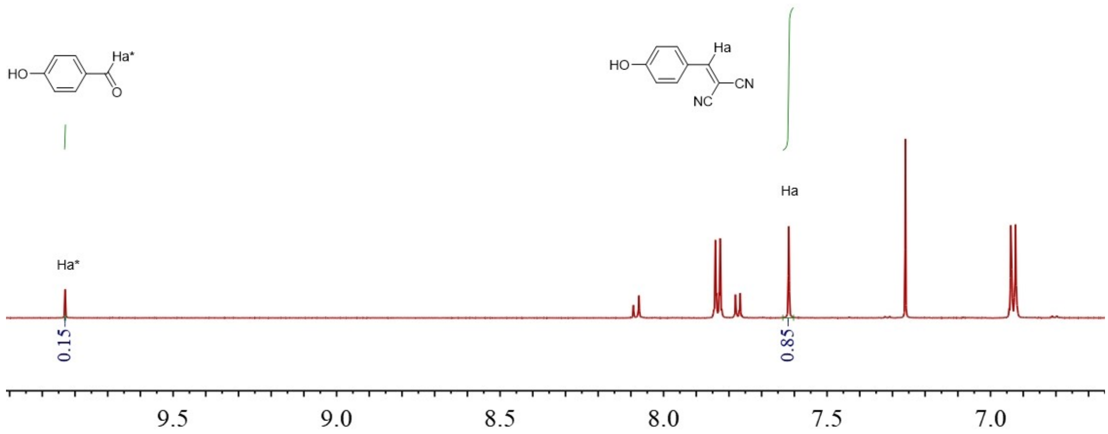

Fig. S37 The comparison of ^{1}H NMR spectra of 4-hydroxybenzaldehyde and its related catalytic product. (Yield: 85 % **Table 5** entry 7).

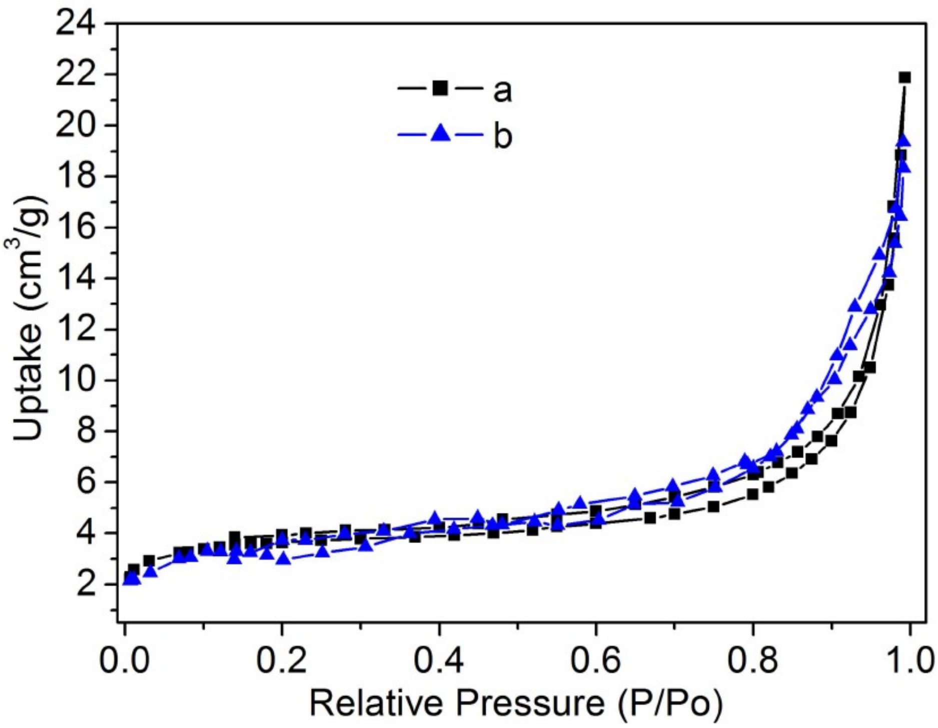

Fig. S38 N_2 adsorption isotherms of Mn-MOF-**1a** before (a) and after (b) catalytic Knoevenagel condensation reaction of benzaldehyde.

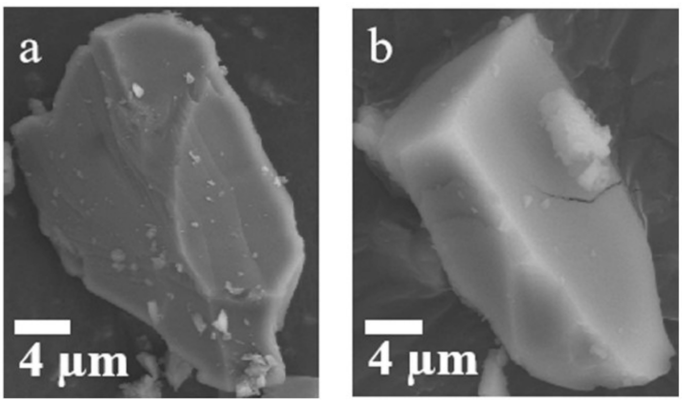

Fig. S39 The SEM imagines of Mn-MOF-**1** before (a) and after (b) catalytic Knoevenagel condensation reaction of benzaldehyde.

References:

S1 Y. Wang, G. P. Yang, P. F. Zhang, L. L. Ma, J. M. Wang, G. P. Li and Y. Y. Wang, *Cryst. Growth Des.*, 2021, **21**, 2734-2743.

S2 C. Yao, S. L. Zhou, X. J. Kang, Y. Zhao, R. Yan, Y. Zhang and L. L. Wen, *Inorg. Chem.*, 2018, **57**, 11157-11164.

S3 H. T. Chen, L. M. Fan and X. T. Zhang, *ACS Appl. Mater. Interfaces.*, 2020, **12**, 54884-54892.

S4 H. T. Chen, T. Zhang, S. R. Liu, H. X. Lv, L. M. Fan and X. T. Zhang, *Inorg. Chem.*, 2022, **61**, 11949-11958.

S5 H. J. Li, X. Y. Zhang, K. Huang and D. B. Qin, *Polyhedron*, 2022, **220**, 115850.

S6 J. Zhang, M. Zou, Q. Li, W. L. Dai, D. Wang, S. Q. Zhang, B. Li, L. X. Yang, S. L. Luo and X. B. Luo, *Appl. Surf. Sci.*, 2022, **572**, 151408.

S7 K. Huang, Q. Li, X. Y. Zhang, D. B. Qin and B. Zhao, *Cryst. Growth Des.*, 2022, **22**, 6531-6538.

S8 Y. H. Chai, Y. Zhao, X. Y. Liu, Z. Y. Cui, B. T. Zhao and L. F. Ma, *Cryst. Growth Des.*, 2022, **22**, 5559-5570.

S9 H. T. Chen, L. M. Fan, T. P. Hu and X. T. Zhang, *Inorg. Chem.*, 2021, **60**, 7276-7283.

S10 H. R. Tian, S. M. Liu, Z. Zhang, T. Y. Dang, Y. Lu and S. X. Liu, *ACS Sustain. Chem. Eng.*, 2021, **9**, 4660-4667.

S11 H. T. Chen, L. M. Fan, T. P. Hu and X. T. Zhang, *Inorg. Chem.*, 2021, **60**, 3384-3392.

S12 X. Y. Cheng, L. R. Guo, H. Y. Wang, J. Z. Gu , Y. Yang, M. V. Kirillova and A. M. Kirillov, *Inorg. Chem.*, 2022, **61**, 17951-17962.

S13 J. B. Deng, X. Wang, Z. Q. Ni and F. Zhu, *Arab. J. Chem.*, 2022, **13**, 7482-7489.

S14 Y. Y. Zhang, Q. Liu, L. Y. Zhang, Y. M. Bao, J. Y. Tan, N. Zhang, J. Y. Zhang and Z. J. Liu, *Dalton. Trans.*, 2021, **50**, 647-659.

S15 G. Q. Huang, J. Chen, Y. L. Huang, K. W, D. Luo, J. K. Jin, J. Zheng, S. H. Xu and W. G. Lu, *Inorg. Chem.*, 2022, **61**, 8339-8348.

S16 A. Paul, L. M. D. R. S. Martins, A. Karmakar, M. L. Kuznetsov, A. S. Novikov, M. F. C. G. D. Silva and A. J. L. Pombeiro, *J. Catal.*, 2020, **385**, 324-337.

S17 A. Das, N. Anbu, A. Dhakshinamoorthy and S. Biswas, *Microp. Mesop. Mater.*, 2019, **284**, 459-467.